Activation of the subventricular zone in multiple sclerosis: Evidence for early glial progenitors

Brahim Nait-Oumesmar*†‡, Nathalie Picard-Riera*†, Christophe Kerninon*†‡, Laurence Decker*†, Danielle Seilhean*†‡, Günter U. Höglinger†§, Etienne C. Hirsch†§, Richard Reynolds¶, and Anne Baron-Van Evercooren*†‡‖

*Institut National de la Santé et de la Recherche Médicale, Unité 546, 75013 Paris, France; †Université Pierre et Marie Curie–Paris 6, 75013 Paris, France; ‡Assistance Publique–Hôpitaux de Paris, Hôpital Pitié-Salpêtrière, Fédération de Neurologie, 75013 Paris, France; §Institut National de la Santé et de la Recherche Médicale, Unité 679, 75651 Paris, France; and ¶Department of Cellular and Molecular Neuroscience, Imperial College London, London W6 8RF, United Kingdom

Edited by Stanley B. Prusiner, University of California, San Francisco, CA, and approved January 9, 2007 (received for review August 10, 2006)

In multiple sclerosis (MS), oligodendrocyte and myelin destruction lead to demyelination with subsequent axonal loss. Experimental demyelination in rodents has highlighted the activation of the subventricular zone (SVZ) and the involvement of progenitor cells expressing the polysialylated form of neural cell adhesion molecule (PSA-NCAM) in the repair process. In this article, we studied the distribution of early PSA-NCAM$^+$ progenitors in the SVZ and MS lesions in human postmortem brains. Compared with controls, MS SVZ showed a 2- to 3-fold increase in cell density and proliferation, which correlated with enhanced numbers of PSA-NCAM$^+$ and glial fibrillary acidic protein-positive (GFAP$^+$) cells. PSA-NCAM$^+$ progenitors mainly were Sox9$^+$, and a few expressed Sox10 and Olig2, markers of oligodendroglial specification. PSA-NCAM$^+$ progenitors expressing Sox10 and Olig2 also were detected in demyelinated MS lesions. In active and chronic active lesions, the number of PSA-NCAM$^+$ progenitors was 8-fold higher compared with chronic silent lesions, shadow plaques, and normal-appearing white matter. In active and chronic active lesions, PSA-NCAM$^+$ progenitors were more frequent in periventricular lesions (30–50%) than in lesions remote from the ventricular wall. These data indicate that, as in rodents, activation of gliogenesis in the SVZ occurs in MS and suggest the mobilization of SVZ-derived early glial progenitors to periventricular lesions, where they could give rise to oligodendrocyte precursors. These early glial progenitors could be a potential target for therapeutic strategies designed to promote myelin repair in MS.

myelin | neural stem cells | remyelination | transcription factors | demyelination

Multiple sclerosis (MS), the most frequent chronic neurological disease of young adults, is characterized by multifocal inflammatory demyelination. Immune-mediated events are assumed to cause loss of myelin and death of oligodendrocytes, leading subsequently to axonal injury (1). Demyelinated plaques can be remyelinated, but this remyelination is not sufficient to overcome disease progression (2, 3). A number of studies have identified mature and immature oligodendrocytes (4–6) and oligodendrocyte precursors (5, 7, 8) in some chronic MS lesions. However, most of these cells are at a quiescent state, and their origin remains unclear.

The subventricular zone (SVZ) of the lateral ventricles, one of the largest germinative area of the adult brain, is characterized by the presence of multipotential cells with persistent proliferation, in rodents (9–11), nonhuman primates (12, 13), and humans (14). Importantly, the rodent SVZ has the ability to generate immature cells capable of long-distance migration (15). In rodent models of neuronal disorders such as seizure, ischemia, or trauma, the SVZ is expanded and neural precursors are mobilized by the lesion, where they differentiate into neurons or astrocytes (16). However, in rodent models of toxin-induced demyelination and inflammatory demyelination, SVZ cells are recruited by the lesion, where they differentiate into glial cells, particularly oligodendrocytes (17–20).

The SVZ persists in the adult human brain and harbors cells expressing the same markers as in rodents, such as the polysialylated form of neural cell adhesion molecule (PSA-NCAM), glial fibrillary acidic protein (GFAP), nestin, and the epidermal growth factor receptor (21, 22). Adult human SVZ cells retain the capacity to self-renew and generate neurons, astrocytes, and oligodendrocytes *in vitro* (23, 24). Despite these similarities, the adult human SVZ differs from rodents in its cellular organization. It is composed merely of a ribbon of GFAP$^+$ presumptive stem cells that are separated from the ependyma by a hypocellular gap and is devoid of chain-migrating neuroblasts (14, 25). Recently, several groups demonstrated that the adult human SVZ is a site of major modifications in response to neurological diseases. Proliferation and neurogenesis are increased in the SVZ of patients with Huntington's disease (26), Alzheimer's disease (27), and epilepsy (28) but are reduced in the SVZ of patients with Parkinson's disease as a result of dopamine depletion (29). However, oligodendrogenesis never was demonstrated in this structure.

Because in MS, the periventricular white matter often is the site of intense inflammation and incomplete remyelination (30), we investigated in postmortem MS brains whether the SVZ is altered and could be a source of newly generated glial progenitors for myelin repair.

Results

Cellular Organization of the SVZ in MS. To investigate the ability of the human SVZ to be reactivated in response to MS, we compared the MS SVZ with that of nonneurological controls. Because the human SVZ is heterogeneous in size and composition (21, 25), we restricted our study to the central body of the SVZ, facing the caudate nucleus and including the striatal vein (Fig. 1*A–C*). This precise location was found only in five controls devoid of neurological diseases and 7 of 17 MS cases. We first investigated whether the cellular organization of the gap be-

Author contributions: B.N.-O. and N.P.-R. contributed equally to this work. B.N.-O., N.P.-R., and A.B.-V.E. designed research; B.N.-O., N.P.-R., C.K., L.D., and D.S. performed research; G.U.H., E.C.H., and R.R. contributed new reagents/analytic tools; B.N.-O., N.P.-R., and A.B.-V.E. analyzed data; and B.N.-O., N.P.-R., and A.B.-V.E. wrote the paper.

The authors declare no conflict of interest.

This article is a PNAS direct submission.

Abbreviations: MS, multiple sclerosis; SVZ, subventricular zone; PSA-NCAM, polysialylated form of neural cell adhesion molecule; GFAP, glial fibrillary acidic protein; PCNA, proliferating cell nuclear antigen; MOG, myelin oligodendrocyte glycoprotein; NAWM, normal-appearing white matter; EAE, experimental allergic encephalomyelitis.

‖To whom correspondence should be addressed at: Institut National de la Santé et de la Recherche Médicale, Unité 546, CHU Pitié-Salpêtrière, 105 Boulevard de l'Hôpital, 75013 Paris Cedex 13, France. E-mail: baron@ccr.jussieu.fr.

This article contains supporting information online at www.pnas.org/cgi/content/full/0606835104/DC1.

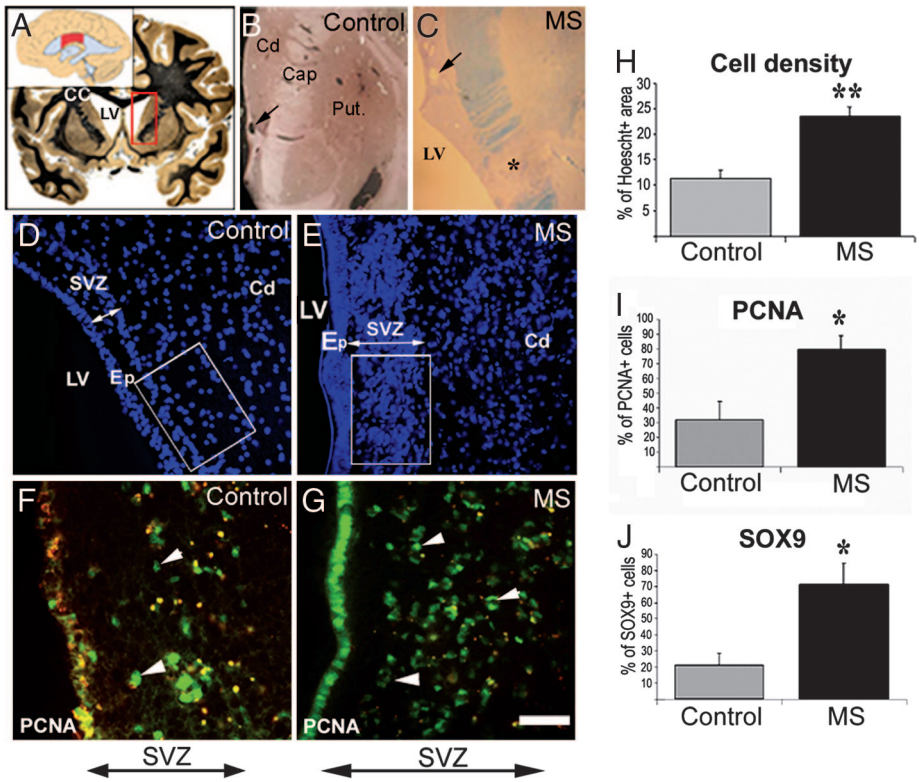

Fig. 1. Increased cell density and proliferation in the SVZ of MS cases. (*A*) Coronal human brain section illustrating the location of the SVZ analyzed. The SVZ lining the lateral ventricle is studied at the level of the caudate nucleus. The central body of the SVZ (red box) is indicated in *Inset*. (*B* and *C*) Higher magnification of the boxed area in *A* for control (*B*) and MS brain (*C*). The arrow indicates the striatal vein. A lesion (asterisk) is identified by Luxol fast blue staining in the internal capsule in *C*. (*D* and *E*) Control and MS brain sections counterstained with the nuclear dye Hoechst 33342. The SVZ thickness is indicated by double arrows. (*F* and *G*) Control and MS brain sections, through the lateral SVZ, stained for PCNA (arrowheads). (*H* and *I*) Evaluation of cell density, proliferation, and Sox9 expression in control and MS SVZ. (*H*) Percentage of Hoechst$^+$ area measured in the boxed area as indicated in *D* and *E*. (*I* and *J*) Percentage of PCNA$^+$ and Sox9$^+$ cells in control and MS SVZ (double arrow). *, $P < 0.001$; **, $P < 0.01$. Cd, caudate nucleus; Put, putamen; LV, lateral ventricle; Cap, internal capsule; CC, corpus callosum; Ep, ependyma. (Scale bars: *B* and *C*, 2 mm; *D* and *E*, 90 μm; *F* and *G*, 45 μm.)

tween the ependymal cell layer and the GFAP$^+$ stem cell ribbon was preserved (14). Hoechst labeling confirmed the presence of the ependymal–stem cell gap in all controls (Fig. 1*D*). In MS tissues, the stem cell ribbon and the gap were filled consistently with Hoechst-labeled nuclei (Fig. 1*E*), with a 2.5-fold increase in cell density over controls (Fig. 1*H*). Therefore, we investigated whether proliferation of SVZ cells was increased in MS brains compared with controls. Proliferating cell nuclear antigen (PCNA), which labels cell nuclei in G_1 and S phases (25), showed a 3-fold increase in cell proliferation in MS SVZ compared with controls (Fig. 1 *F*, *G*, and *I*).

We performed immunohistochemistry with specific markers to define the expanded population. The expression of GFAP (Fig. 2 *A–C*) and PSA-NCAM (Fig. 2 *D–F*) were increased drastically in the SVZ of MS compared with controls. Confocal three-dimensional reconstitution of the MS SVZ showed that the enlarged GFAP$^+$ population and processes alternated with layers of PSA-NCAM$^+$ cells, suggesting that GFAP$^+$ cells encompassed PSA-NCAM$^+$ cells [supporting information (SI) Fig. 6]. Chain migration was not observed in control or MS SVZ. However, in MS brains, GFAP$^+$ or PSA-NCAM$^+$ progenitors with a unipolar or bipolar morphology were found oriented in a tangential or perpendicular plane to the lateral ventricle wall, suggesting their migration along or away from the SVZ (Fig. 2 *C* and *F*). We further characterized the expanded SVZ population by using antibodies against transcription factors such as Sox9, Sox10, and Olig2, which are involved in oligodendrogenesis (31–34). Rare Sox9-expressing cells were present in the control SVZ. Their number increased 3-fold in MS compared with controls (Fig. 1*J*), and most of these cells coexpressed GFAP (Fig. 2 *G* and *H*) or PSA-NCAM (Fig. 2*I*). Sox10$^+$ and Olig2$^+$ cells also were found in the SVZ. Although few of these cells coexpressed PSA-NCAM (Fig. 2 *J* and *K*), their majority was labeled for NG2 (Fig. 2 *L* and *M*). Because Olig2 also is involved in neurogenesis (32, 34), we investigated the possibility that these cells would express the neuroblast marker β3-tubulin (35). Although few β3-tubulin$^+$ cells were detected in the control (25) and MS SVZ, colabeling of Olig2 and β3-tubulin rarely was detected (data not shown). Because of the limited number of comparable SVZ cases, definitive conclusions on potential fluctuations of Sox10$^+$ or Olig2$^+$ progenitors between MS and controls could not be reached.

Detection of PSA-NCAM-Expressing Cells in MS Lesions. In rodents, PSA-NCAM$^+$ progenitors of the SVZ and RMS can be recruited by nearby demyelinated lesions (19). We thus explored whether such progenitors were present in MS lesions. Lesions were identified macroscopically and confirmed by using anti-myelin oligodendrocyte glycoprotein (MOG) (Fig. 3 *A* and *B*) or anti-myelin basic protein antibodies. Because PSA-NCAM is known to be expressed by reactive astrocytes after CNS injury (19, 36), we performed immunolabeling for PSA-NCAM and GFAP. Two types of cells expressing PSA-NCAM were identified. The predominant PSA-NCAM$^+$ population had a stellar shape, coexpressed GFAP (Fig. 3*C*), and was distributed widely in MS and normal-appearing white matter (NAWM). These cells were assumed to be reactive astrocytes and were excluded from further analysis. The second population had a round shape,

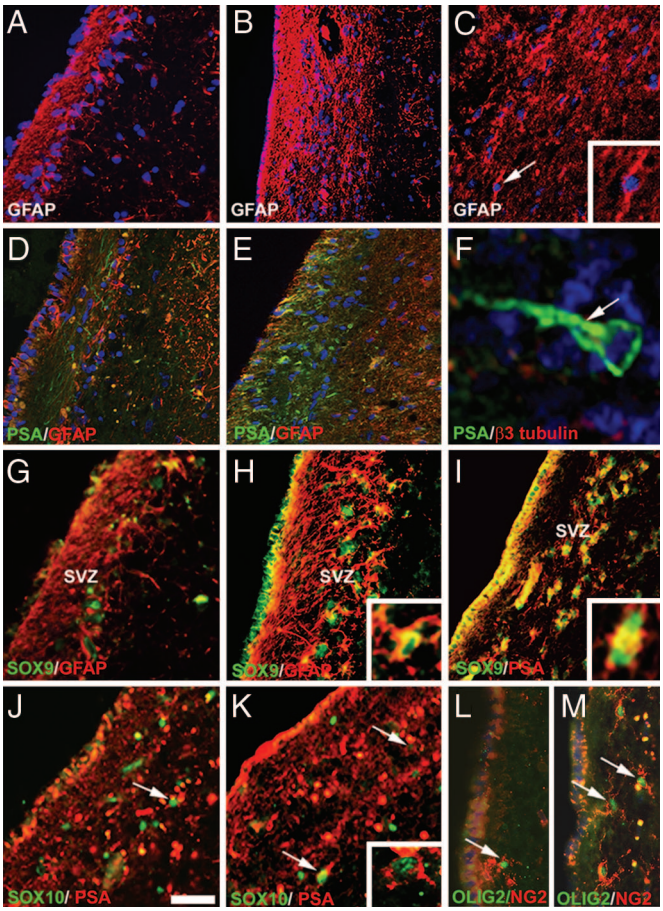

Fig. 2. Cellular changes of the SVZ in MS. (*A* and *B*) GFAP expression is highly increased in the MS SVZ (*B*), and the gap is filled with GFAP processes compared with control (*A*). (*C*) Detection of GFAP$^+$ cells with a bipolar morphology in MS SVZ (*Inset*). (*D* and *E*) Only few PSA-NCAM$^+$ neuronal processes are present in the control SVZ (*D*), whereas numerous round PSA-NCAM$^+$ progenitors are observed in the gap of MS SVZ (*E*). (*F*) PSA-NCAM$^+$ cells (arrow) with a unipolar morphology leaving the SVZ. (*G* and *H*) Expression of Sox9 and GFAP in control (*G*) and MS SVZ (*H*). (*I*) Colocalization of Sox 9 in PSA-NCAM$^+$ progenitors in MS SVZ. (*J* and *K*) Few PSA-NCAM$^+$ progenitors (arrows) express Sox10 in control (*J*) and MS SVZ (*K*). (*L* and *M*) Detection of cells coexpressing Olig2 and NG2 in the gap of control (*L*) and MS SVZ (*M*). The lateral ventricle is at the left side of each image. *A–F* are counterstained with Hoechst 33342. (Scale bars: *A–E* and *G–M*, 45 μm; *F*, 10 μm; *C Inset*, 20 μm; *K Inset*, 12 μm.)

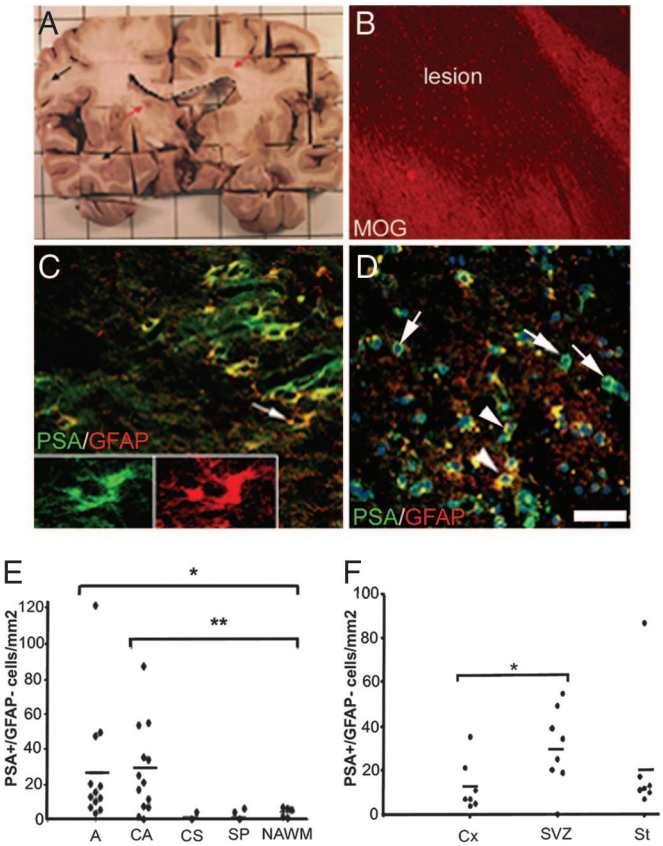

Fig. 3. Identification of PSA-NCAM$^+$ progenitors in MS lesions. (*A*) Periventricular (red arrow) and nonperiventricular (black arrow) lesions and the lateral ventricle (dotted lines) are detectable macroscopically in a slice of MS brain. (*B*) Identification of a lesion by anti-MOG immunolabeling. (*C* and *D*) Detection of PSA-NCAM$^+$ cells in lesions. (*C*) PSA-NCAM$^+$ cells with a stellar shape express GFAP. Arrow indicates the cell represented in the *Inset*. (*D*) A second population of PSA-NCAM$^+$ cells has round shapes and is mostly GFAP$^-$ (arrows) with few GFAP$^+$ (arrowheads). (*E* and *F*) Quantification of PSA-NCAM$^+$ progenitors in MS lesions. Their density is increased significantly in active and chronic active lesions compared with NAWM (*E*; *, $P < 0.05$; **, $P < 0.01$) and in lesions localized near the ventricle compared with cortical lesions (*F*; *, $P < 0.05$). *D* is counterstained with Hoechst 33342. A, active; CA, chronic active; CS, chronic silent; SP, shadow plaque; Cx, cortex; St, striatum. (Scale bars: *B*, 170 μm; *C* and *D*, 45 μm; *Insets*, 20 μm.)

generally did not express GFAP (Fig. 3*D* and 4*E*), and was localized mainly within MS lesions and periplaque white matter. Based on their shape, we considered them to be PSA-NCAM$^+$ progenitors. We next evaluated the density of PSA-NCAM$^+$ round progenitors according to the lesion activity. Quantification showed that PSA-NCAM$^+$ progenitors were significantly more abundant in active (26.99 $\pm$ 9.63 cells per mm^2) and chronic active (27.33 $\pm$ 7.08 cells per mm^2) lesions compared with chronic silent lesions (2.09 $\pm$ 2.09 cells per mm^2), shadow plaques (3.35 $\pm$ 1.82 cells per mm^2), or NAWM (4.05 $\pm$ 1.16 cells per mm^2) (Fig. 3*E*). We also analyzed the correlation between the numbers of PSA-NCAM$^+$ progenitors in active and chronic active lesions and their proximity to the SVZ. The number of PSA-NCAM$^+$ progenitors was higher in lesions proximal to the SVZ than in lesions moderately (striatum) or far-remote (cortex, two blocks away) from the SVZ, with mean densities of 30 cells per mm^2 in lesions proximal to the SVZ, 22 cells per mm^2 in striatal lesions, and 13 cells per mm^2 in cortical lesions (Fig. 3*F*).

The plasticity of PSA-NCAM$^+$ progenitors and their preferential location in areas of adult neurogenesis led us to perform coimmunolabeling for PSA-NCAM and early neuronal and oligodendroglial markers in active ($n = 12$) and chronic active ($n = 13$) lesions (Fig. 4 *A–D*). Although some axonal sprout-like structures coexpressed PSA-NCAM and β3-tubulin (37), the majority of PSA-NCAM$^+$ progenitors were not stained for β3-tubulin (Fig. 4*A*). Because active, and to a lesser extent, chronic active lesions contain substantial numbers of macrophages, we excluded the possibility that these PSA-NCAM$^+$ cells were macrophages by immunolabeling for CD68 (Fig. 4*B*). To investigate their glial identity, we next analyzed coexpression of PSA-NCAM and Sox9, Sox10, Olig2, and NG2. PSA-NCAM$^+$ progenitors did not stain for Sox9, but few of them expressed Sox10 (Fig. 4*C*) or Olig2 (Fig. 4*D*). Ramified NG2$^+$ cells, which did not stain for PSA-NCAM, also were present in these lesions (data not shown). PSA-NCAM$^+$ progenitors often appeared as closely apposed doublets (Fig. 4*E*). We thus evaluated their potential for proliferation with the anti-Ki67 antibody. Most Ki67$^+$ cells were located in NAWH. In lesions, Ki67$^+$ cells mainly were immune cells located in peri- or vascular spaces, and few were parenchymal PSA-NCAM$^+$ progenitors (Fig. 4*F*).

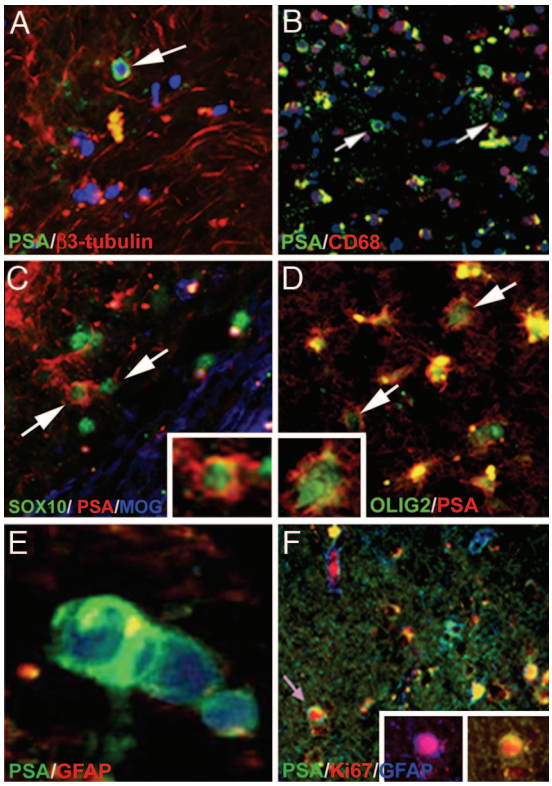

Fig. 4. Characterization of PSA-NCAM$^+$ round progenitors in MS lesions. (*A* and *B*) PSA-NCAM$^+$ progenitors (arrow) do not express the neuronal marker β3-tubulin (*A*) or the macrophage marker CD68 (*B*) in MS lesions. (*C* and *D*) Few PSA-NCAM$^+$ progenitors (arrows) stain for Sox10 (*C*) and Olig2 (*D*). The edge of the lesion is identified by MOG immunolabeling (blue in *C*). (*E*) Doublet of presumably dividing PSA-NCAM$^+$ cells. (*F*) Ki67$^+$ progenitor (arrow) double-stained for GFAP and PSA-NCAM (*Inset*). *A*, *B*, and *E* are counterstained ng with Hoechst 33342. (Scale bars: *A*, *B*, and *F*, 45 μm; *C* and *D*, 22 μm; *E*, 6 μm; *D Inset*, 10 μm; *F Inset*, 20 μm.)

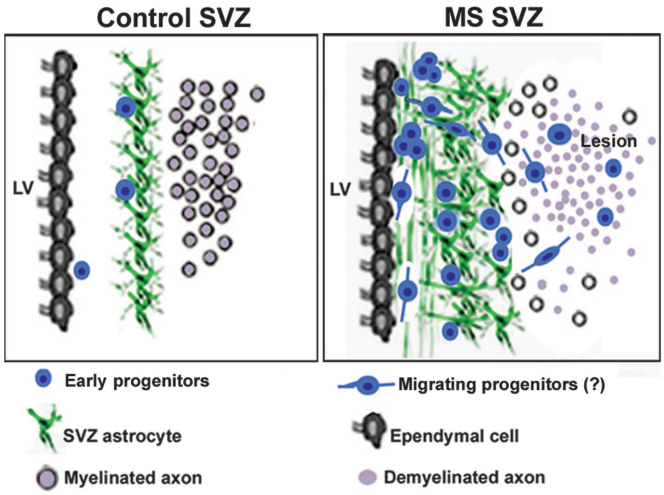

Fig. 5. Proposed model illustrating the activation of the SVZ in MS. The control SVZ is composed of a ribbon of GFAP$^+$ astrocytes separated from the ependymal wall by a hypocellular gap, containing few early progenitors. In MS SVZ, the density of GFAP$^+$ astrocytes and early progenitors is increased. These progenitors express early glial markers such as Sox9, Sox10, and Olig2 in the subependymal region. Similar progenitors prevail in periventricular lesions. The presence of PSA-NCAM$^+$ progenitors with a bipolar morphology suggest their potential migration within or away from the SVZ. These data suggest the mobilization of SVZ-derived early progenitors to periventricular lesions, where they could contribute to oligodendrocyte renewal.

These observations indicated that some PSA-NCAM$^+$ progenitors retained the capacity to proliferate and generate new oligodendrocyte precursors and astrocytes in active and chronic active lesions.

Discussion

In this study, we present evidence of activation of the SVZ in MS, leading to the generation of PSA-NCAM$^+$ progenitors in the ependymal–stem cell region. Early progenitors also were found in periventricular MS lesions. Expression of early markers such as Sox9, Sox10, and Olig2 by PSA-NCAM$^+$ progenitors revealed their commitment to a glial rather than neuronal fate. The prevalence of PSA-NCAM$^+$ progenitors in lesions proximal to the SVZ as well as the detection of progenitors with bipolar profiles suggest that some of them migrate into nearby lesions where they could be one of the sources of the previously described oligodendrocyte progenitors (6, 38) (Fig. 5).

Our data showed a clear expansion of the SVZ, based on the increase in cell density and proliferation in MS groups compared with controls. This finding is similar to experimental models of ischemia, seizure, or demyelination in rodents and nonhuman primates, showing a strong correlation between SVZ expansion and increased cell proliferation (39–42). Enhanced proliferation in the SVZ also was found in experimental allergic encephalomyelitis (EAE) mice, a model of MS (19). Although the average disease duration in EAE mice lasted 18 days, the average disease duration is 30 years in MS and thus 10-fold longer than in EAE when reported to the mean lifespan of each species. These observations suggest that the prolonged exposure to repetitive inflammatory insults did not fully exhaust the proliferative potential of the SVZ and maintained most progenitors at an immature stage. Although patient age (43 years) and disease course could affect proliferation in the SVZ as well, the limited age and disease type variation among our MS patients did not permit us to establish such a correlation.

The adult human SVZ is composed of GFAP$^+$ stem cells, ependymal cells, and rare PSA-NCAM$^+$ cells (25). In the MS SVZ, the majority of PSA-NCAM$^+$ progenitors expressed Sox9, a transcription factor involved in the switch of neural stem cells from neurogenesis to gliogenesis (31). The round shape and the expression of Sox9 indicate that the PSA-NCAM$^+$ progenitors were at a very immature stage. The presence of transient amplifying cells, defined by Olig2 expression in the rodent SVZ (43), has not been described so far in humans. We showed that few Olig2$^+$/NG2$^+$ cells are present in the gap of controls and MS SVZ. In view of their location and their lack of expression of neuronal markers, these cells may represent the transient amplifying population. However, some cells coexpressed Olig2 and Sox10, suggesting their commitment to the oligodendroglial lineage.

The nature and mode of action of the signals reactivating the SVZ in MS and animal models are unknown. SVZ expansion seems to be a common phenomenon of diseases characterized by inflammation (26–28). However, the genesis of specific cell types points to the presence of disease-specific signaling events (i.e., demyelination in MS). Recent data suggest that the cerebrospinal fluid flow plays a critical role in directional migration (44) or proliferation of SVZ precursors in rodents (45). Because the cerebrospinal fluid in MS is the site of many molecular and cellular modifications (46) and ependymal and GFAP$^+$ cells are tightly connected with each other (14, 25, 47), it is tempting to speculate that each cell type contributes to the SVZ reactivation by retrieving information from their respective environments.

PSA-NCAM$^+$ progenitors also were detected in MS lesions and prevailed in active and chronic active lesions. They were found in higher numbers in lesions close to the SVZ than in more

remote ones. In addition, a subpopulation of cells with bipolar profiles was found to be oriented in the radial or tangential plane of the ventricular wall. Although chain migration never was observed, these observations suggest that PSA-NCAM$^+$ progenitors in MS lesions near the lateral ventricle could arise from the SVZ, as in rodents (19). However, the existence of a population of endogenous progenitors in the white matter (48–50) that could be activated at the early stage of the disease should not be excluded because PSA-NCAM$^+$ progenitors also were identified in lesions remote from the SVZ.

This study has identified a population of early progenitors expressing PSA-NCAM in the SVZ and in active and chronic active MS lesions. Although these cells do not prevent the long-term disease progression, they do represent highly interesting therapeutic targets to potentially stimulate endogenous myelin repair.

Materials and Methods

Tissue. Brain tissue blocks from neuropathologically confirmed MS were provided by the U.K. Multiple Sclerosis Tissue Bank at Imperial College London. Tissues were collected with the donors' fully informed consent via a prospective donor scheme after ethical approval by the London Multicenter Research Ethics Committee (MREC 02/2/39; London, U.K.). Neurologically normal control ($n = 5$) tissues were collected from the Parkinson's Disease Tissue Bank at the Pitié-Salpêtrière Hospital (Paris, France) or the U.K. Multiple Sclerosis Tissue Bank. Seventeen cases of randomly chosen MS were studied, including primary progressive (PP, 3 cases), secondary progressive (SP, 12 cases), relapsing-remitting (RR, 1 case), and relapsing progressive (RP, 1 case), (SI Table 1). The average duration of disease since the onset of the first symptoms was 28 years (range 8–39 years). The mean age was 57 years (range 38–77 years) for MS patients and 58 years (range 27–95 years) for controls. The mean death-tissue preservation delay was 11 h (range 7–19 h) in MS cases and 22 h (range 9–56 h) in controls.

Classification of MS Lesions. Digital photography of freshly dissected brain coronal sections was used to define the precise anatomical location of the 2-cm × 2-cm lesion-containing blocks. Lesions ($n = 30$) were classified according to the inflammatory activity and as described in refs. 51 and 52. NAWM samples ($n = 5$) were selected far from the lesions, in blocks with normal myelin staining, cortical lesions ($n = 7$) were at least two blocks apart from the SVZ, SVZ lesions ($n = 8$) were adjacent to the lateral SVZ, and striatal lesions ($n = 7$) were within the internal capsule (Fig. 1*C* and 3*A*).

Histology and Immunohistochemistry. Dissected MS and control brains were cut into 2-cm × 2-cm blocks, fixed for 7 days in 4% paraformaldehyde in PBS, cryoprotected, frozen, and stored at −85°C. Ten-micrometer-thick sections were cut on a cryostat and mounted on gelatin-coated slides for analysis. The locations of the lesions were identified with Luxol fast blue staining. For immunohistochemistry, the primary antibodies used were as follows: mouse IgG2a anti-MOG antibody (1/1,000; clone Z12; S. Piddlesden, University of Cardiff, Cardiff, U.K.), guinea pig IgG anti-MBP antibody (1/100; ref. 11), mouse IgG1 anti-CD68 antibody (1/100; Dako, Glostrup, Denmark), mouse IgM anti-PSA-NCAM antibody (1/100; Abcys, France), mouse IgG1 anti-GFAP antibody (1/100; Chemicon, Hampshire, U.K.), rabbit anti-NG2 antibody (1/100; Chemicon), mouse IgG2a anti-β3-tubulin antibody (1/200; Sigma–Aldrich, Lyon, France), mouse IgG1 anti-PCNA antibody (1/500; Dako), mouse IgG1 anti-Ki67 (1/100; Dako), rabbit IgG anti-Olig2 (1/100; IBL, Gunma, Japan), and guinea pig IgG anti-Sox9 and anti-Sox10 (1/50; R&D Systems, Abingdon, U.K.). Secondary antibodies were FITC- or TRITC-conjugated. Slides were mounted with Fluoromount (Electron Microscopy Sciences, Hatfield, PA) and analyzed with a DMRB fluorescence microscope or SP2 AOBS confocal microscope (Leica, Wetzlar, Germany).

Quantitative Analysis. Quantification of PSA-NCAM$^+$/GFAP$^-$ cells inside MS lesions was performed on digital images of four serial sections (100-μm apart). The number of Sox9$^+$, PCNA$^+$ cells and the density of Hoechst$^+$ nuclei in the body of the lateral SVZ from MS ($n = 7$) and controls ($n = 5$) was evaluated at the level of the caudate nucleus (Fig. 1 *A–D*) (25). Cell counts were performed with the ImageJ software in defined microscopic fields (0.08 mm^2). Counts of PCNA$^+$ and Sox 9$^+$ cells were expressed as a percentage of the total cell population in the SVZ, and counts of Hoechst$^+$ cells were expressed as pixel values per mm^2 on a minimum of four serial coronal sections per SVZ. Every coimmunostaining was verified further by confocal microscopy.

Statistics. Data are expressed as the mean ± SEM. Nonparametric statistical tests were performed (Student's t test) with GraphPad PRISM software (GraphPad Software, Inc., San Diego, CA). The results were determined to be significant when $P < 0.05$.

We are grateful to the U.K. and French MS tissue banks, the Pitié-Salpêtrière Imaging Plate-form for their technical assistance, and H. Baron for critically reviewing the manuscript. This work was supported by grants from the National Multiple Sclerosis Society (Award TR 3762-A-1), Institut National de la Santé et de la Recherche Médicale/Association Française contre les Myopathies–Cellules Souches Adultes, and Association de Recherche sur la Sclérose en Plaques. N.P.-R. received a fellowship from the Recherche Médicale Foundation, and C.K. received a fellowship from the European Leukodystrophy Foundation.

1. Raine CS, Cross AH (1989) *Lab Invest* 60:714–725.
2. Prineas JW, Connell F (1978) *Neurology* 28:68–75.
3. Lassmann H, Bruck W, Lucchinetti C, Rodriguez M (1997) *Mult Scler* 3:133–136.
4. Kuhlmann T, Lucchinetti C, Zettl UK, Bitsch A, Lassmann H, Bruck W (1999) *Glia* 28:34–39.
5. Wolswijk G (1998) *J Neurosci* 18:601–609.
6. Chang A, Tourtellotte WW, Rudick R, Trapp BD (2002) *N Engl J Med* 346:165–173.
7. Scolding NJ, Rayner PJ, Sussman J, Shaw C, Compston DA (1995) *NeuroReport* 6:441–445.
8. Scolding N, Franklin R, Stevens S, Heldin CH, Compston A, Newcombe J (1998) *Brain* 121:2221–2228.
9. Luskin MB (1993) *Neuron* 11:173–189.
10. Altman J (1969) *J Comp Neurol* 137:433–457.
11. Lachapelle F, Avellana-Adalid V, Nait-Oumesmar B, Baron-Van Evercooren A (2002) *Mol Cell Neurosci* 20:390–403.
12. Pencea V, Bingaman KD, Freedman LJ, Luskin MB (2001) *Exp Neurol* 172:1–16.
13. Kornack DR, Rakic P (2001) *Science* 294:2127–2130.
14. Sanai N, Tramontin AD, Quinones-Hinojosa A, Barbaro NM, Gupta N, Kunwar S, Lawton MT, McDermott MW, Parsa AT, Manuel-Garcia Verdugo J, *et al.* (2004) *Nature* 427:740–744.
15. Lois C, Alvarez-Buylla A (1994) *Science* 264:1145–1148.
16. Picard-Riera N, Nait-Oumesmar B, Baron-Van Evercooren A (2004) *J Neurosci Res* 76:223–231.
17. Nait-Oumesmar B, Decker L, Lachapelle F, Avellana-Adalid V, Bachelin C, Van Evercooren AB (1999) *Eur J Neurosci* 11:4357–4366.
18. Decker L, Durbec P, Rougon G, Evercooren AB (2002) *Mol Cell Neurosci* 19:225–238.
19. Picard-Riera N, Decker L, Delarasse C, Goude K, Nait-Oumesmar B, Liblau R, Pham-Dinh D, Evercooren AB (2002) *Proc Natl Acad Sci USA* 99:13211–13216.
20. Menn B, Garcia-Verdugo JM, Yaschine C, Gonzalez-Perez O, Rowitch D, Alvarez-Buylla A (2006) *J Neurosci* 26:7907–7918.
21. Bernier PJ, Vinet J, Cossette M, Parent A (2000) *Neurosci Res* 37:67–78.
22. Weickert CS, Webster MJ, Colvin SM, Herman MM, Hyde TM, Weinberger DR, Kleinman JE (2000) *J Comp Neurol* 423:359–372.

23. Roy NS, Wang S, Jiang L, Kang J, Benraiss A, Harrison-Restelli C, Fraser RA, Couldwell WT, Kawaguchi A, Okano H, *et al*. (2000) *Nat Med* 6:271–277.
24. Kukekov VG, Laywell ED, Suslov O, Davies K, Scheffler B, Thomas LB, O'Brien TF, Kusakabe M, Steindler DA (1999) *Exp Neurol* 156:333–344.
25. Quinones-Hinojosa A, Sanai N, Soriano-Navarro M, Gonzalez-Perez O, Mirzadeh Z, Gil-Perotin S, Romero-Rodriguez R, Berger MS, Garcia-Verdugo JM, Alvarez-Buylla A (2006) *J Comp Neurol* 494:415–434.
26. Curtis MA, Penney EB, Pearson AG, van Roon-Mom WM, Butterworth NJ, Dragunow M, Connor B, Faull RL (2003) *Proc Natl Acad Sci USA* 100:9023–9027.
27. Jin K, Galvan V, Xie L, Mao XO, Gorostiza OF, Bredesen DE, Greenberg DA (2004) *Proc Natl Acad Sci USA* 101:13363–13367.
28. Crespel A, Rigau V, Coubes P, Rousset MC, de Bock F, Okano H, Baldy-Moulinier M, Bockaert J, Lerner-Natoli M (2005) *Neurobiol Dis* 19:436–450.
29. Hoglinger GU, Rizk P, Muriel MP, Duyckaerts C, Oertel WH, Caille I, Hirsch EC (2004) *Nat Neurosci* 7:726–735.
30. Patrikios P, Stadelmann C, Kutzelnigg A, Rauschka H, Schmidbauer M, Laursen H, Sorensen PS, Bruck W, Lucchinetti C, Lassmann H (2006) *Brain* 129:3165–3172.
31. Stolt CC, Lommes P, Sock E, Chaboissier MC, Schedl A, Wegner M (2003) *Genes Dev* 17:1677–1689.
32. Lu QR, Sun T, Zhu Z, Ma N, Garcia M, Stiles CD, Rowitch DH (2002) *Cell* 109:75–86.
33. Wegner M, Stolt CC (2005) *Trends Neurosci* 11:583–588.
34. Zhou Q, Anderson DJ (2002) *Cell* 109:61–73.
35. Doetsch F, Garcia-Verdugo JM, Alvarez-Buylla A (1997) *J Neurosci* 17:5046–5061.
36. Oumesmar BN, Vignais L, Duhamel-Clerin E, Avellana-Adalid V, Rougon G, Baron-Van Evercooren A (1995) *Eur J Neurosci* 7:480–491.
37. Charles P, Reynolds R, Seilhean D, Rougon G, Aigrot MS, Niezgoda A, Zalc B, Lubetzki C (2002) *Brain* 125:1972–1979.
38. Wolswijk G (2002) *Brain* 125:338–349.
39. Parent JM, Valentin VV, Lowenstein DH (2002) *J Neurosci* 22: 3174–3188.
40. Takasawa K, Kitagawa K, Yagita Y, Sasaki T, Tanaka S, Matsushita K, Ohstuki T, Miyata T, Okano H, Hori M, Matsumoto M (2002) *J Cereb Blood Flow Metab* 22:299–307.
41. Zhang RL, Zhang ZG, Zhang L, Chopp M (2001) *Neuroscience* 105:33–41.
42. Arvidsson A, Collin T, Kirik D, Kokaia Z, Lindvall O (2002) *Nat Med* 8:963–970.
43. Hack MA, Saghatelyan A, de Chevigny A, Pfeifer A, Ashery-Padan R, Lledo PM, Gotz M (2005) *Nat Neurosci* 8:865–872.
44. Sawamoto K, Wichterle H, Gonzalez-Perez O, Cholfin JA, Yamada M, Spassky N, Murcia NS, Garcia-Verdugo JM, Marin O, Rubenstein JL, *et al*. (2006) *Science* 311:629–632.
45. Owen-Lynch PJ, Draper CE, Mashayekhi F, Bannister CM, Miyan JA (2003) *Brain* 126:623–631.
46. Wekerle H (1998) *Mult Scler* 4:136–137.
47. Spassky N, Merkle FT, Flames N, Tramontin AD, Garcia-Verdugo JM, Alvarez-Buylla A (2005) *J Neurosci* 25:10–18.
48. Arsenijevic Y, Villemure JG, Brunet JF, Bloch JJ, Deglon N, Kostic C, Zurn A, Aebischer P (2001) *Exp Neurol* 170:48–62.
49. Nunes MC, Roy NS, Keyoung HM, Goodman RR, McKhann G, II, Jiang L, Kang J, Nedergaard M, Goldman SA (2003) *Nat Med* 9:439–447.
50. Windrem MS, Nunes MC, Rashbaum WK, Schwartz TH, Goodman RA, McKhann G, Roy NS, Goldman SA (2004) *Nat Med* 10:93–97.
51. Lucchinetti CF, Bruck W, Rodriguez M, Lassmann H (1996) *Brain Pathol* 3:259–274.
52. Lassmann H (1998) *Mult Scler* 3:93–98.